Earthquake Engineering, Tenth World Conference © 1992 Balkema, Rotterdam. ISBN 90 5410 060 5

Shaking table test on ultimate behavior of seismic isolation system Part 2: Response behavior of rubber bearings

Katsuhiko Ishida & Hiroo Shiojiri
Central Research Institute of Electric Power Industry, Abiko, Japan

Genji Yoneda
Takenaka Corporation, Tokyo, Japan

Atsuo Matsuda
Okumura Corporation, Tsukuba Research Institute, Japan

ABSTRACT: Recently studies on a seismic isolation system have actively been carried out and many base isolated structures have been constructed in the world. However, there are still some problems which have yet to be clarified for the ultimate response behavior and the seismic safety margin of base isolated structures, when they are subjected to a seismic force beyond the design base earthquake. Therefore, with the aim of understanding these phenomena, the shaking table tests were conducted. The test models were supported by eight sets of lead rubber bearings. Excitation tests were carried out repeatedly through the gradual increase of the acceleration of the input motion to the shaking table. The rubber bearings were not ruptured until the input level reached approximately 6.5 times the tentative design earthquake. As a result obtained from the tests, it was confirmed that the base isolation system which was designed in this study possessed a sufficient seismic safety margin.

1. INTRODUCTION

The outline of the tests and the response behavior of the superstructures were described in PART 1. As was show in PART 1, the superstructure is a reinforced concrete rigid body with a weight of 174.4 kN (17.8 tons). In order to investigate the influence of the overturning moment of the superstructure upon the ultimate response behavior of the laminated rubber bearings, two test models with a low and a high center of gravity were adopted. The ratios of the height of the gravity center to the model width were 0.5 and 0.25. These models were supported by eight sets of lead rubber bearings which were a 1/15 scaled model of the prototype bearing. The tentative design wave, whose velocity response spectrum of a damping ratio of 5% is set at 100 kine in the range of 2 to 10 seconds in period, is defined as S1 earthquake in this study. In the shaking table tests it was reduced in time to $1/\sqrt{15}$ according to the similarity rule. This paper will explain both the ultimate response behavior and the rupturing state of the lead rubber bearings (LRBs), which were seen when excitation was repeatedly imposed while gradually increasing the input acceleration of the tentative design wave.

2. TEST RESULTS

2.1 Ultimate Response Behavior of the Laminated Rubber Bearings

Fig. 1 shows the relationship between the shearing force of the LRBs and the horizontal relative displacement in Case-A (a model with a low center of gravity). The value of the shearing force in the figure is an average of the shearing force of the eight rubber bearings. The broken lines indicate the result of the

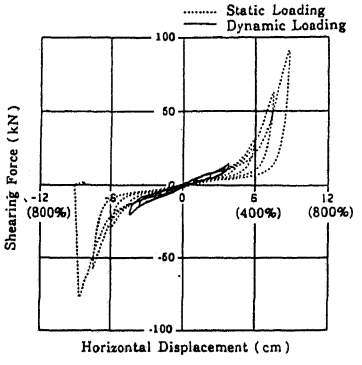

a) at the level of 3.0S1

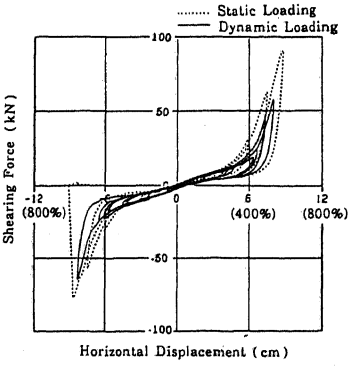

b) at the level of 6.0S1

Fig.1 Relationship Between Shearing Force and Horizontal Displacement (Case - A)

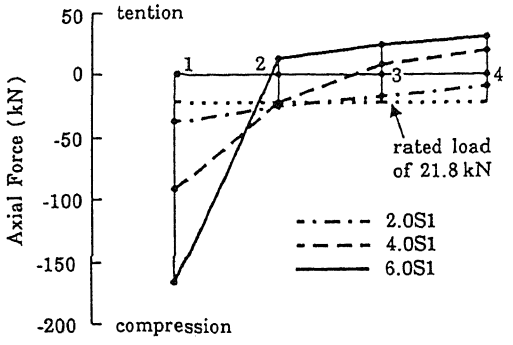

Fig. 2 Axial Force Distribution when Compression Force of 1st Street Rubber Bearing is Maximum (Case-A)

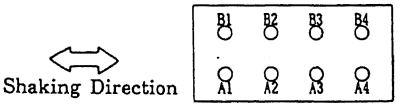

static cyclic failure test of the LRB which was carried out under the condition that a rated axial load of 21.8 kN was added (See Ref. 1). At the level of 3.0 S1, the maximum shearing strain of the LRB is 289%, and a slight hardening tendency can be seen in the hysteresis loop. In the shaking table tests, excitation was performed twelve times within the range between 3.0 S1 and 6.0 S1 through increasing the intensity of the input acceleration by 0.25 S1 each time. As a result, compared with the hysteresis loop of the stasic failure tests, the stiffness of the LRBs degrades in the hardening region at 6.0 S1. This is due to the influence exerted by the cyclic exitation. However, the hysteresis loop shows stable characteristics regardless of the cyclic loading.

Fig. 2 shows the axial force distribution at each input level. The rocking center is positioned at the center of the test model when the input level is low. The tensile stiffness of the LRB is much smaller than the compressive stiffness. Therefore, when the tensile force acts on the LRBs with the increase of the input level, the rocking center moves to the edge of the model. In the case of inputing 6.0 S1, only the LRBs at

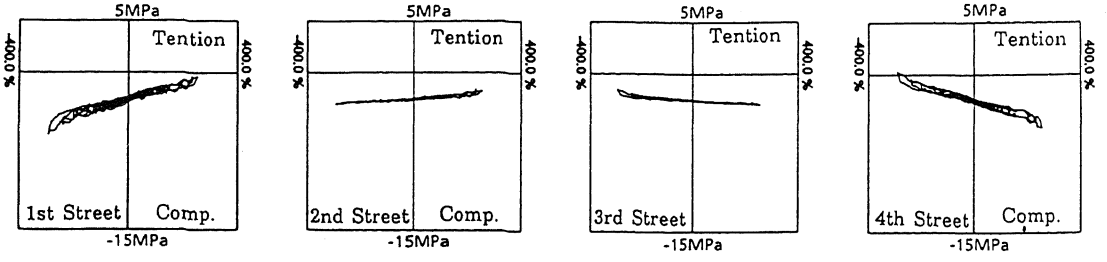

a) at the level of 3.0S1 for the Model with a Low Center of Gravity

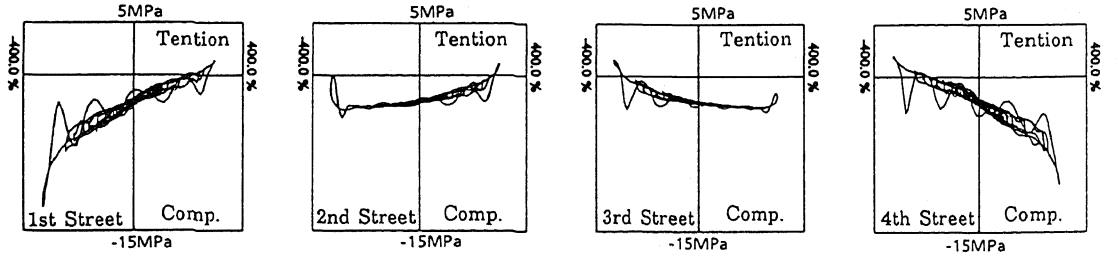

b) at the level of 3.0S1 for the Model with a High Center of Gravity

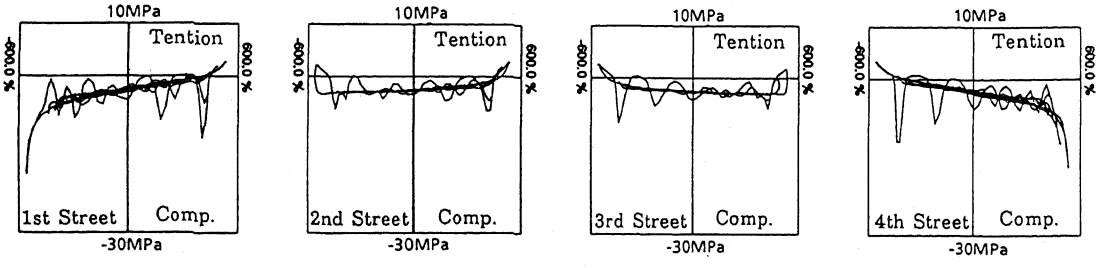

c) at the level of 6.0S1 for the Model with a Low Center of Gravity

Fig.3 Relationship Between Axial Stress and Shearing Strain

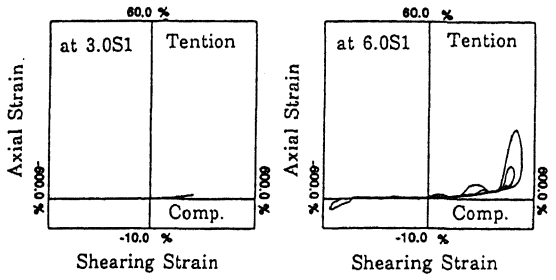

a) Model with a Low Center of Gravity

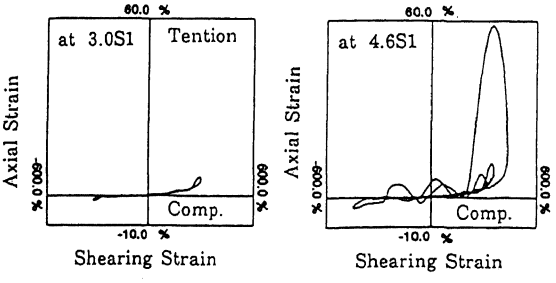

b) Model with a High Center of Gravity

Fig.4 Axial Strain - Shearing Strain Relationship (A-4 LRB)

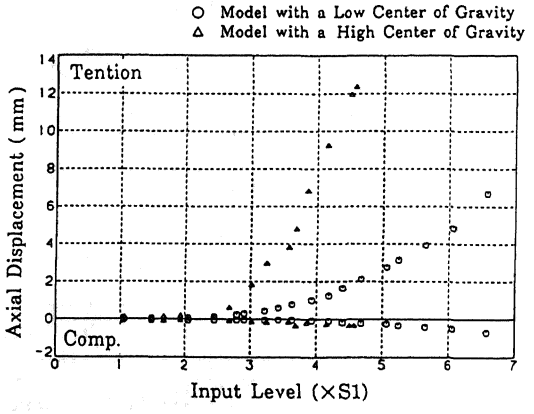

Fig.5 Comparison of the Maximum Vertical Displacement at 4th Street by the Height of the Center of Gravity

the edge are compressive. Due to the movement of the rocking center toward the edge, a vertical response vibration is induced. Fig. 3 shows the relationship between the axial stress and the shearing strain of the LRBs. The variation of the axial stress for the LRBs installed at the edge is larger than that for the inner ones. At the level of 6.0 S1, the hysteresis loop for the model with a low center of gravity indicated in Fig. 3 becomes wavy because of the up-lift and drop of the superstructure. On the contrary, the hysteresis loop for the model with a high center of gravity begins to wave at the level of 3.0 S1. It is recognized that the

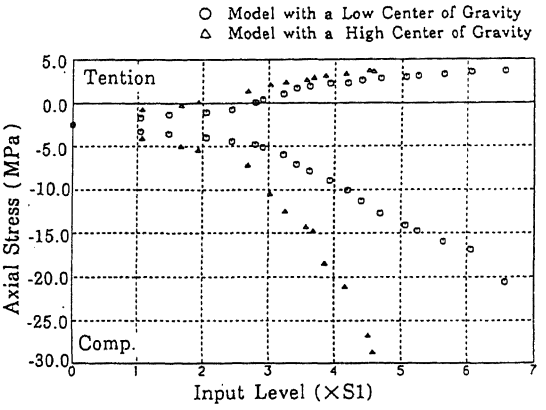

Fig.6 Comparison of the Maximum Axial Force at 4th Street by the Height of the Center of Gravity

influence of the rocking vibration exerted upon the model with a high center of gravity is much greater than that for the model with a low center of gravity. When the input level is low and the rocking center is positioned at the center of the model, the axial stress is linearly related to the shearing strain. On the contrary, when the input level becomes large, the compressive axial force largely increases just around an area where the shearing strain becomes maximum. This occurs due to both the fact that the increasing ratio of the shearing strain reduces as the LRBs reach a hardening region, and that the rocking center moves toward the edge of the model.

Fig. 4 shows the relationship between the axial strain and the shearing strain for the LRB at A-4. Just around a region where the shearing strain becomes maximum, the tensile strain caused by the up-lift of the model largely increases. Furthermore, when the laminated rubber bearings are subjected to shearing deformation, their effective bearing area for the vertical load is reduced and the compressive stiffness decreases. Therefore, the compression strain increases in large shearing strain region.

Fig. 5 and 6 show the maximum vertical relative displacement and the axial stress at each input level. At the level of 2.5 S1 or less, the response value in a vertical direction is small and the differences caused by the height of the center of gravity are hardly seen. However, when the input level is greater than 2.5 S1, the response value in a vertical direction rapidly increases. This is caused by the following. First, the response acceleration of the superstructure increases due to the fact that the hysteresis loop of the LRBs reaches a hardening region and the horizontal stiffness becomes high when the input level is greater than 2.5 S1. Secondly, at the level of 2.5 S1 or more, tensile force starts to act on the LRBs and the rocking vibration becomes larger. The tensile strain for the model with a low center of gravity is 32% at 6.0 S1, and that for the model with a high center of gravity is 82% at 4.6 S1. Furthermore, the compressive axial force of the model with a high center of gravity is approximately double that of the model with a low center of gravity. When 4.6 S1 is input, a compressive stress of 27.8 MPa (11.4 times the rated loading stress

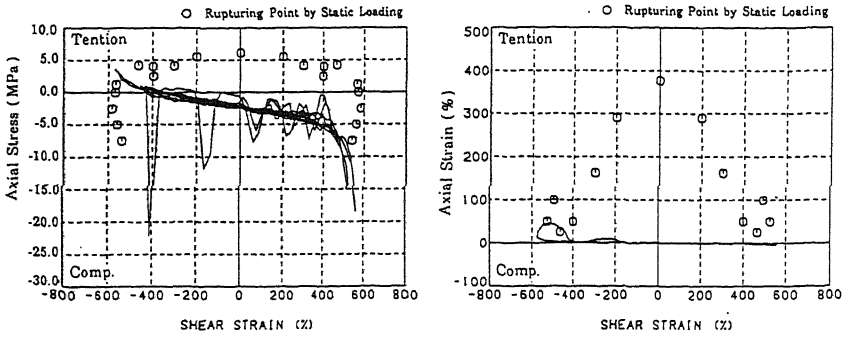

(Axial Stress - Shearing Strain Relationship) (Axial Strain - Shearing Strain Relationship)

a) Hysteresis during the Last Exitation before the Rupture

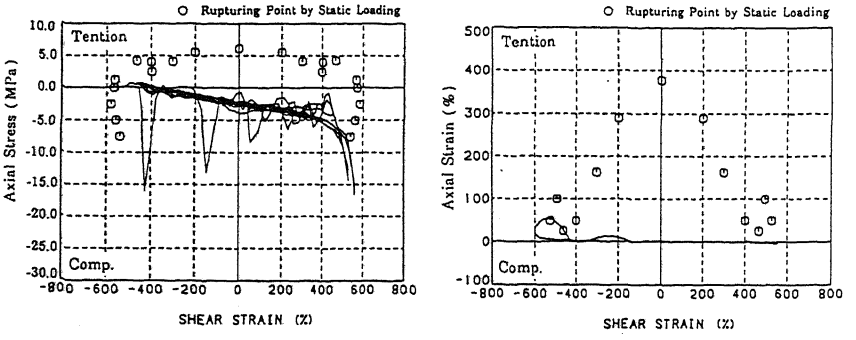

(Axial Stress - Shearing Strain Relationship) (Axial Strain - Shearing Strain Relationship)

b) Hysteresis during the Rupturing Exitation

Fig.7 Hysteresis Curves of the A-4 LRB in Case A Compared with the Rupturing Point by Static Loading

of 2.45 MPa) acts on the LRB of the model with a high center of gravity.

Therefore, from the view point of the seismic safety margin, the model with a low center of gravity was more advantageous than that with a high center of gravity. And it would be recommended that the tensile force should not act on the laminated rubber bearings under the design base earthquake.

2.2 Rupturing State of the Laminated Rubber Bearings

The following will explain the rupturing state for the laminated rubber bearings.

1) For Case-A, at the level of 6.5 S1, the A-4 rubber bearing was ruptured. For Case-C, after the A-4 rubber bearing fractured first at the level of 6.6 S1, three laminated rubber bearings ruptured at each repeated excitation in the order of B-4, A-1 and A-3. Both Case-A and Case-C are models with a low center of gravity. Since the LRBs installed at the edge of the model are more influenced by the rocking vibration, they are ruptured more easily than the inner ones. In the case of the model with a high center of gravity, the vertical response acceleration became too large with the increase of the rocking vibration. Then, the emergency stop device on the shaking table operated and it was impossible to continue adding excitation until the laminated rubber bearings ruptured.

2) Only one bearing was ruptured during each excitation. No evidence was observed that the rupture of one bearing of LRB would cause a chain-reaction rupture of other bearings.

3) The shearing strain when the LRBs ruptured was approximately 600%. For the full-sized laminated rubber bearing the shearing strain at the rupture is about 450% (See Ref. 2). The LRBs used in this test are 1/15 scaled models of the prototype LRBs for which the rated capacity is 4900 kN, and their diameter is only 107 mm. So, the rupturing shear strain is approximately 1.3 times that for the full-sized laminated rubber bearings.

4) The rupturing state of LRBs was observed using a video. In regard to the four pieces out of the five LRBs which ruptured, the local failure occured from either the upper or lower edge of the LRB, when they were under the compressive state, after then they completely ruptured under the tensile state. Only the A-3 rubber bearing for Case-C suddenly fractured under the tensile state without previously cracking. When the compressive axial force acts on the LRB which is subjected to shearing deformation, the local strain at the upper and lower edge of the LRB becomes larger due to the influence of the bending moment. On the contrary, when the tensile force acts on the LRB, the local strain is relieved under the condition of low

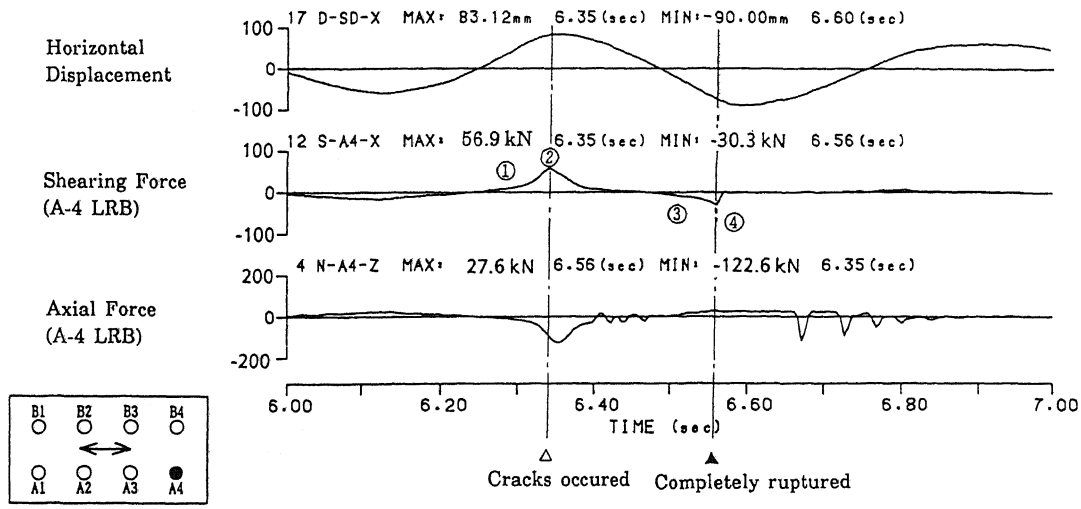

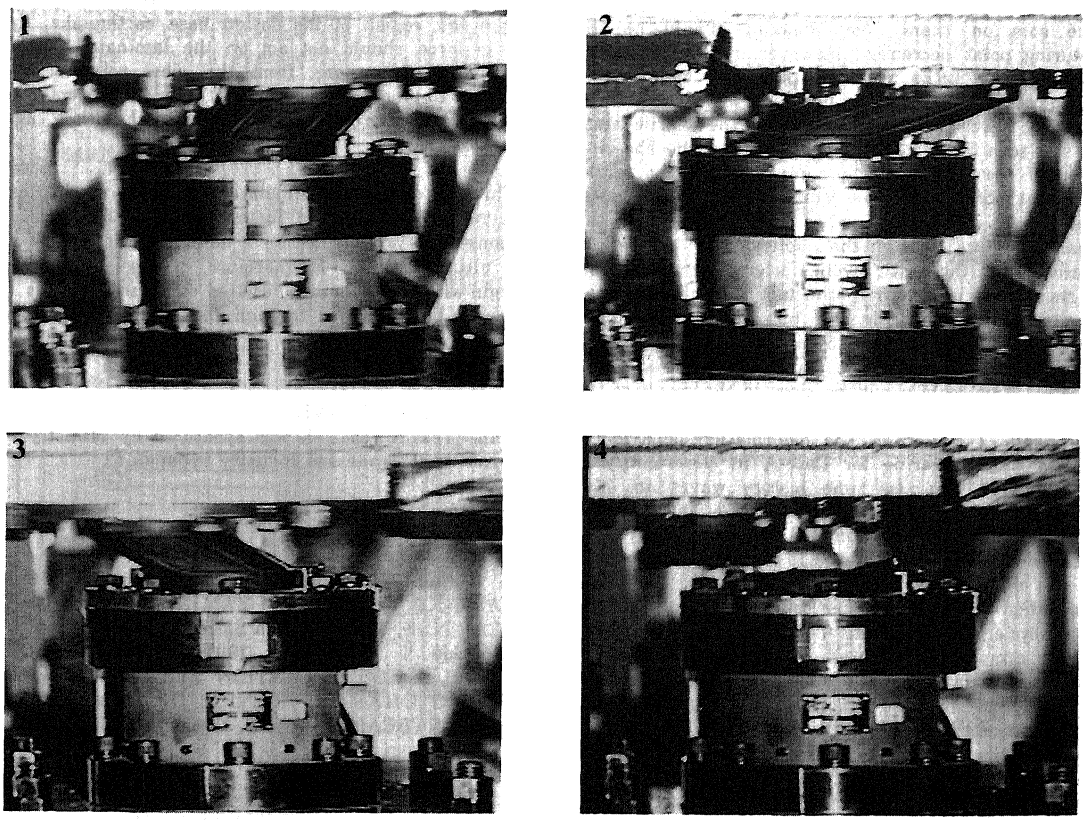

Photo. ① LBR is going to deform to the right hand under the compression state

Photo. ② Cracks had occured at the lower left side

Photo. ③ LBR is going to deform to the left hand under the tensile state

Photo. ④ Completely ruptured

Photo. 1 Deformation Behavior of A-4 LRB for Cace-A in the Vicinity of the Rupturing Time

tensile strain. It is considered this is one of the reasons why most of the local failure occured under the compressive state.

5) Fig. 7 indicates the hysteresis loop of the A-4 rubber bearing for Case-A (a model with a low center of gravity) at the rupturing time and that at the previous excitation. The input level for both cases is 6.5 S1. In the same figure, the rupturing points obtained from the static tests which were carried out in advance through the use of the LRBs with the same shape and dimensions are also plotted (See Ref. 1). The static tests were conducted through the application of static cyclic loading. In the static tests, with an increase of the compressive axial force, the shearing strain at the rupture becomes slightly smaller. It can be considered that this is caused due to the deviation of the test specimens. According to other studies (Ref. 2), in regard to the laminated rubber bearings with the same geometry as the LRBs used in this test, the shearing strain at the rupturing point should be almost constant, even if a compressive axial stress of approximately ten times the rated loading stress of 2.45 MPa acts on it. On the contrary, as the tensile force acts on them, the shearing strain at the rupturing point decreases. However, since the tensile strain of the LRBs is comparatively small in the shaking table tests, the phenomenon in which the rupturing shear strain lowers under the tensile state was not seen. In the shaking table tests, the shearing strain of the LRBs at the rupturing point is larger than that observed in the static cyclic failure tests. Therefore, it is conservative in safety to estimate the dynamic rupture through the application of the results obtained from the static cyclic failure tests. However, we should pay attention to the fact that the response velocity becomes faster in this test, because the input motion is reduced to $1/\sqrt{15}$ in time. So, it can be considered that the dynamic rupturing shear strain in an actual time scale would be close to the result of the static cyclic failure tests.

6) Photo. 1 illustrates the deformation behavior of the A-4 rubber bearing for Case-A in the vicinity of the rupturing time. Its time history waves are also shown in Photo. 1. Although the inside of the LRB can not be observed on account of the covering rubber sheet, cracks had occured at 6.35 seconds at the lower left side of the A-4 rubber bearing. Photo. ② shows the deformation of the A-4 rubber bearing at that time. At a half cycle after that (at 6.55 sec), the A-4 rubber bearing completely ruptured as shown in Photo. ④. Photo. ①,② shows the A-4 rubber bearing under the compressive state, and Photo. ③,④ illustrates the bearing under the tensile state. When the time history wave of the shearing force on the LRBs was investigated, it was clarified that even if the LRB was damaged as shown in Photo. ② it transmitted the same shearing force as that of undamaged rubber bearings. The laminated rubber bearing did not completely rupture under the state shown in Photo. ② because the horizontal deformation was quickly released in the dynamic tests. This is considered to be one of the reasons why the shearing strain at the rupturing point becomes larger than that observed in the static cyclic failure tests.

3. CONCLUSIONS

A shaking table test on the ultimate behavior of the base isolated structures was carried out. The test model was supported by eight sets of lead rubber bearings. The results which have been obtained from the tests are summarized as follows.

1) The laminated rubber bearings were not ruptured until a seismic motion with a level of 6.5 times the tentative design wave was input. Therefore, the seismic isolation system designed in this study has a sufficient seismic safety margin.

2) It was observed that when a piece of the laminated rubber bearing ruptured, it did not cause rupturing in the other pieces.

3) The rupturing shear strain in the shaking table test was larger than the static rupturing strain. Therefore, it is conservative in safety to estimate the dynamic rupture through the results obtained from the static cyclic failure tests.

4) When the laminated rubber bearings reached a tensile region by the rocking vibration, the vertical response was greatly increased. Therefore, at least within the region of the design base earthquake, the tensile force should not act on the laminated rubber bearings. Furthermore, from the view point of the seismic safety margin, the model with a low center of gravity was more advantageous than that with a high center of gravity.

Through conducting simulation analyses of the test results, it is planned to further develop the ultimate response analysis method for a base isolation system at the ultimate state. Furthermore, the seismic safety margin which actual base isolated structures possess is going to be evaluated through the application of this response analysis method.

ACKNOWLEDGEMENTS

This present research was sponsored by Ministry of International Trade and Industry in Japan.

REFERENCES

1) K. Ishida, H. Shiojiri, M. Iizuka et al. 1991. FAILURE TESTS OF LAMINATED RUBBER BEARINGS, Trans. of 11th SMIRT K25/5

2) T.Mazda, T. Fujita et al. 1991. TEST ON LARGE-SCALE SEISMIC ISOLATION ELEMENTS Part 2 STATIC CHARACTERISTICS OF LAMINATED RUBBER BEARING TYPE, Trans. of 11th SMIRT K25/4